Microbial Fuel Cell: Study of Bioresource Potential of Dairy Effluent and Associated Process Limitations

Umair Fazal
Center for Energy Research and Development, UET Lahore, 54890, Pakistan
AN Tabish (antabish@uet.edu.pk)
University of Engineering and Technology https://orcid.org/0000-0001-5803-1510
Samina Akbar
Center for Energy Research and Development, UET Lahore, 54890, Pakistan
Iqra Farhat
Center for Energy Research and Development, UET Lahore, 54890, Pakistan
Muneed Irshad
Department of Physics, UET Lahore, 54890, Pakistan
Mohsin Kazmi
Department of Chemical Engineering, UET Lahore, 54890, Pakistan
Haider Ali
Department of Chemical Engineering, UET Lahore, 54890, Pakistan
Muhammad Irfan
Department of Chemical Engineering, UET Lahore, 54890, Pakistan

Research

Keywords: MFC, EIS, Biofilm, Bioelectricity, Wastewater treatment

Posted Date: March 13th, 2021

DOI: https://doi.org/10.21203/rs.3.rs-285485/v1

Microbial Fuel Cell: Study of Bioresource Potential of Dairy Effluent and Associated Process Limitations

Umair Fazal [a], Asif N. Tabish [a,b,*], Samina Akbar [c], Iqra Farhat [a], Muneeb Irshad [d], Mohsin Kazmi [b], Haider Ali [b], Muhammad Irfan [b]

[a] Center for Energy Research and Development, UET Lahore (New Campus), 54890, Pakistan

[b] Department of Chemical Engineering, UET Lahore (New Campus), 54890, Pakistan

[c] Department of Humanities and Basic Sciences, UET Lahore (New Campus), 54890, Pakistan

[d] Department of Physics, UET Lahore, 54890, Pakistan

*Corresponding author: E-mail: antabish@uet.edu.pk

Phone: 03137040288

Abstract:

Microbial fuel cells (MFCs) are devices that exploit the electrochemically active microorganisms for the oxidative conversion of organic compounds into electricity. MFC technology is therefore expected to be a viable solution for domestic and industrial wastewater treatment as an alternative to the currently applied activated-sludge process. Despite its potential, the technology is facing application challenges because of high cost, low stability, and limited understanding of cell design and operation. In this experimental study, a double-chambered MFC with graphite electrodes and a proton-conducting membrane is used in a batch mode to study the potential of resource recovery from dairy effluent and identify the process limitations. Results showed a promising cell performance as the chemical oxygen demand of the wastewater reduced from 4520 mg/l to 850 mg/l in 10 days including the time required for biofilm development. The highest open-circuit voltage of 396 mV was recorded on the third day along with the highest power density of 36.39 mW/m^2 corresponding to a current density of 0.30 A/m^2. Further, the electrochemical impedance spectroscopy revealed that the activation polarization of aerated cathode is the main contributor to cell internal resistance followed by the ohmic resistance.

Keywords: MFC; EIS; Biofilm; Bioelectricity; Wastewater treatment

1. Introduction:

While the wastewater has serious environmental consequences, it also contains varying levels of valuable organic compounds that can be converted to energy, chemicals, and various fuels during the treatment process. The activated sludge process is currently widely applied to treat domestic and industrial wastewater however it has inherent limitations such as high energy consumption and waste sludge production. Therefore, there is a need to develop and adopt sustainable technologies that can treat wastewater and recover resources simultaneously. Microbial fuel cells (MFCs) are novel and sustainable systems that electrochemically convert chemical energy, present between chemical bonds of organic compounds, into electrical energy (Ren et al. 2014; Moradian et al. 2021).

MFCs use microbes as catalysts to oxidize organic matter under anaerobic conditions and in return generate electricity (Santoro et al. 2017). MFC technology can treat wastewater ranging from a simple substrate such as sucrose, glucose, and protein to complex and undefined substrates such as wastewater from domestic and municipal, pharmaceutical, brewery, dairy, food processing, agro-processing livestock, petroleum, and paper recycling industry. The operation of MFC differs from bioremediation, that is the conversion of organic compounds to H_2O and CO_2 under aerobic conditions (Rajasulochana and Preethy 2016). Integration of bioremediation with MFCs can establish synergy between the two processes resulting in enhanced energy recovery, pollutant removal, and resource recovery from high strength wastewater (Vu and Min 2019). The sludge disposal rate and treatment efficiency achieved with MFC technology is comparable or sometimes better than conventional technologies (Wang et al. 2012; Gude 2016).

While MFC is regarded as a sustainable wastewater treatment technology, its commercial application is challenged due to high capital cost, low power density, and a lack of larger-scale module development (Kim et al. 2007; Deval and Dikshit 2013). Electrode materials account for a larger share in the capital cost of MFC systems. While platinum offers the highest electrochemical activity, it is too expensive to be used for

commercial applications (Zhang et al. 2012). Stainless steel has been reported suitable for long-term and large-scale applications due to good conductance, corrosion resistance, and mechanical stability (Erable et al. 2017). Anode modifications with polymers and metal oxides have been employed to enhance the performance of MFC (Chen et al. 2017). Alternatively, carbon-based electrodes in the form of carbon cloth, graphite fiber brush, carbon foam, carbon-nano tubes, and graphene have been reported to exhibit superior performance (Call et al. 2017; Li et al. 2017). It is worth mentioning that carbon is a low-cost and biologically compatible material and can be extracted from indigenous biomass residue. Recent developments focusing on cell configurations and MEA material have helped to overcome shortcomings associated with MFC technology (Slate et al. 2019).

The performance of MFCs is greatly influenced by various factors such as the electron transfer rate from the bacteria to the anode, the ohmic resistance of the electrolyte, diffusion of the substrate into the biofilm, and other electrochemical kinetics (Aghababaie et al. 2015). The non-conductive lipid layers present at the outer portion of the majority of microbial species inhibit direct electron transfer to the anode surface. Therefore, an electron mediator is used to accelerate the electron transfer rate (Schröder 2007). Oxygen reduction reaction (ORR), which requires high reduction potential, can also affect the performance of MFC. To overcome this problem mediators can be used that not only help in the electron transfer mechanism but also lower the reduction potential at the cathode (Sun et al. 2013). In mediator-free MFCs, electrochemically active bacteria transfer the electrons directly to the anode. The microbes such as Shewanella Putrefactions, Aeromonas hydrophilia, and Geobacter are among the electrochemically active bacteria (Bin 2009). To increase the ORR reaction and proton conductivity different electrolytes such as phosphate buffer saline solution, potassium ferricyanide, potassium phosphate, and potassium permanganate phosphate buffer solution are proposed (Nam et al. 2010; Ahn and Logan 2013; Ghazali et al. 2017).

The production of maximum power is limited by high internal resistance known as ohmic, activation, and concentration losses (Varanasi et al. 2017; Yin et al. 2017). To engineer high-performing electrode

materials and cell designs, it is important to quantify each resistance first and then develop loss minimizing stratagem (Hou et al. 2010). While there have been advances in the MFC technology in the last decade regarding developing low-cost electrode materials, optimizing the system performance, and scaling up the application, the understanding of underlying physiochemical processes and the rate-determining steps is limited that can primarily be attributed to the complexity of the systems. This work is therefore undertaken to investigate the resistance offered by various competing processes during wastewater treatment besides determining the potential of resources recovery using low cost graphite electrodes. The internal resistance of an MFC is typically determined by techniques such as current interruption method, power density peak method, and polarization slope method. These techniques require MFC obeying simple Ohm's law which practically is not the case. The highly non-linear behavior of reaction kinetics and mass transport as well as dependence on the operating conditions require spectroscopic techniques such as electrochemical impedance spectroscopy (EIS) (He and Mansfeld 2009). In EIS, the MFC system is perturbed from the equilibrium condition by a small sinusoidal signal, and the way the system follows the response is studied at a steady state. Fitting EIS spectra with an electrical equivalent circuit give the values of resistance, capacitance, and impedance associated with physical and chemical processes (Sindhuja et al. 2016).

The present work has used dual-chamber MFC, with carbon electrodes and anionic membrane, for the treatment of dairy effluent. The data (physical, chemical, and electrochemical) was recorded on 24 hr basis for 10 days with wastewater of an initial COD level of 4520 mg/l to determine the MFC performance and quantify limitations that need to be addressed in the development of MFC technology.

2. Methodology:

2.1. Materials and Construction:

A dual-chamber MFC with 300 mL capacity of each chamber and separated by a heterogeneous anionic membrane (AMI-7001, US international) was used for the experiments. Both of the electrodes were prepared using activated carbon paste. The rationale behind using activated carbon is its low cost and

affinity towards microbes – activated carbon is an optimized material for microbial filtration in commercial wastewater treatment systems. The anodic chamber was completely sealed to maintain the anaerobic condition. The electrons generated in the anodic chamber transfer to the cathodic chamber through an external circuit. Whereas, the proton transfer occurs through the anionic membrane from the cathode to the anode to complete the circuit. The schematic of the setup is shown in Figure 1.

Both anode and a cathode having surface area 12 cm^2 and 15 cm^2, respectively were prepared from carbon paste. The larger area of the cathode favors oxygen reduction reaction (ORR) at the cathode chamber. The carbon paste was prepared by mixing 45 g of graphite, 25 g of activated carbon, and 30 g of paraffin oil (used as a binder) in mortar and castle. Electrodes were washed with the ethanol solution to remove any impurities present. The anode was placed in the anodic chamber and the container was sealed to create anaerobic conditions. To complete the outer circuit, the electrodes were connected with copper wire through potentiostat for electrochemical characterization.

An anode chamber was filled with 250 mL dairy farm effluent simulant. The solution was prepared in the lab by mixing 10 g cow dung and 10 g sugar in 1000 ml of distilled water to get an initial COD value of 4520 mgL^{-1}. The cathode was filled with 250 mL of phosphate buffer Saline solution (PBS). PBS was prepared by adding 0.2 g of KCL, 0.8 g of NaCl, 1.44 g of Na_2HPO_4, and 0.24 g of KH_2PO_4 in 800 mL of distilled water to make a total solution volume of 1000 mL as described in (Medicado AB 2008). The PH of the PBS solution was adjusted at 7.4 with HCL. Aeration was provided in the cathode chamber by a fish pump. Air was introduced near the wall of the cathode chamber to avoid direct contact of bubbles with the electrode however saturating the catholyte. MFC cycle was run in batch mode for 10 days at room temperature.

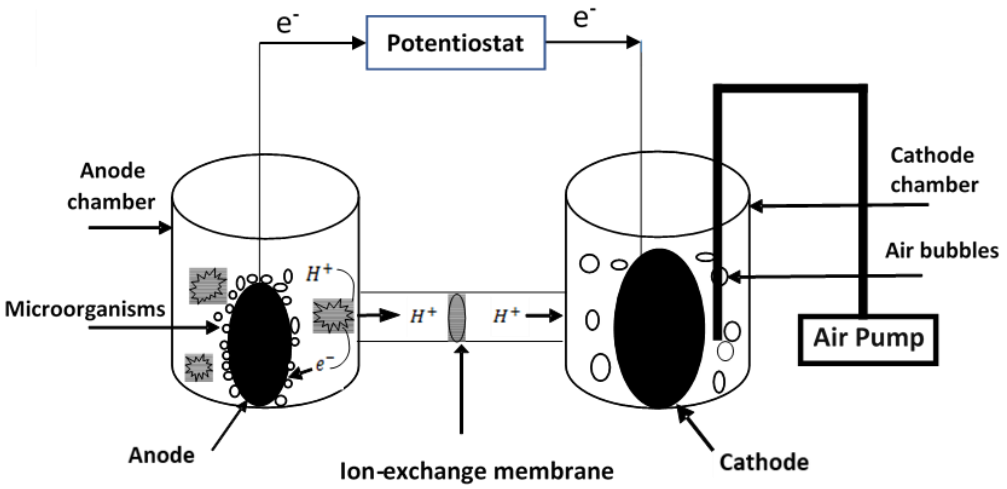

Figure 1: Schematic diagram of Double Chamber Microbial Fuel Cell

2.2. Measurements and analysis:

The wastewater analysis was performed in a batch mode under the ambient temperature of 25 $\pm$ 3 ^{o}C. The PH of the substrate was determined electrometrically using the Hanna instrument. For chemical characterization, chemical oxygen demand (COD) was determined by drawing a 2 ml sample from the anolyte and examining externally using high range COD vials (HI-937540). 0.2 mL of wastewater solution was put into the COD vial and placed in the COD test tube heater for 120 minutes at 150 ^{0}C. After this COD was measured using the Hanna photometer. The COD removal efficiency was calculated as:

$$\text{COD Removal Efficiency} = \frac{COD_f - COD_i}{COD_i} \times 100$$

For electrochemical characterization, Gamry potentiostat (Interface 1000) was used with two-electrode assembly in which the cathode acts as a counter as well as a reference electrode. For the EIS study, the sinusoidal potential of magnitude 10 mV between a frequency range of 0.05 Hz to 100 kHz was applied. The dynamic response of the cell was obtained in the form of Nyquist and Bode plots. The results of EIS were fitted to an electrical equivalent circuit using the Gamry Echem Analyst. I-V curves were obtained

with an applied current range of 0 to 0.002 ampere at a scan rate of 0.005 As^{-1}. The system was given sufficient time (at least 30 minutes) to restore the equilibrium after consecutive measurement.

3. Results and Discussion:

3.1. Chemical analysis of the dairy effluent

The cell was operated for a period of 10 days. Chemical properties like chemical oxygen demand (COD) and the pH of the anolyte solution were measured before and after the cell operation. The initial COD value was found to be 4520 mg L^{-1} which on utilization by microorganisms decreased to 850 mg L^{-1} after 10 days, thereby giving percentage removal of 81% which is in reasonable agreement with the performance of MFC operated with domestic and sewage wastewater (Ghangrekar and Shinde 2008; Logan et al. 2012). The pH of the anolyte decreased from 7.62 to 5.8 which indicates a strong shift from near neutral to acidic behavior. Such behavior was expected as electrochemical oxidation creates an acidic environment inside the solution.

3.2. OCV and polarization study

Figure 2 shows the change in cell voltage for the sample with the initial COD value of 4520 mg/L. It is found that the cell voltage initially increases from 280 mV to a maximum value of 396 mV on the third day and then starts decreasing. The initial increase of power density owing to the increase in cell potential in the first 72 hrs is reported elsewhere as well (Sindhuja et al. 2016). The increase in the voltage in MFC is attributed to biofilm formation at the anode that effectively oxidized the organic matter and decline may be related to the utilization of organic matter (Sathishkumar et al. 2018). The drop in OCV is not more than 10% of the value recorded on day 1. The OCV of 396 mV is comparable with the reported values and indicates the metabolism of organic matter by microorganisms and the formation of biofilm on the anode.

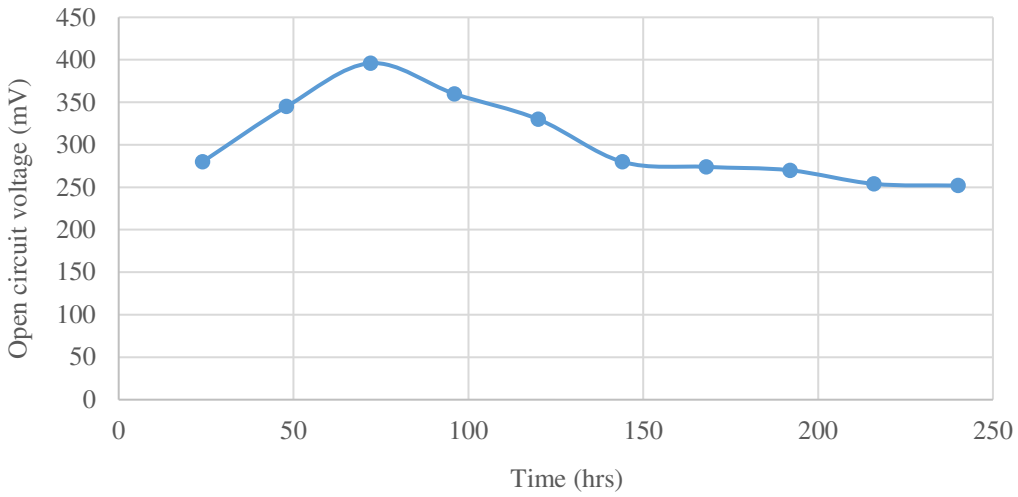

Figure 2: Open circuit voltage

Figure 3 shows the polarization curve. Cell voltage in the polarization curve is seen to decrease monotonically with load, a classical scenario observed during fuel cell operation. Drop in the cell voltage is linked to the losses including activation loss, ohmic loss, and concentration loss. The nearly symmetrical shape of the power density curves suggests that the maximum power is obtained well before the effective substrate consumption takes place. The maximum power density is found to be 36.39 mWm^{-2} that is of the same order of magnitude as reported for various wastewater samples as compared in Table 1.

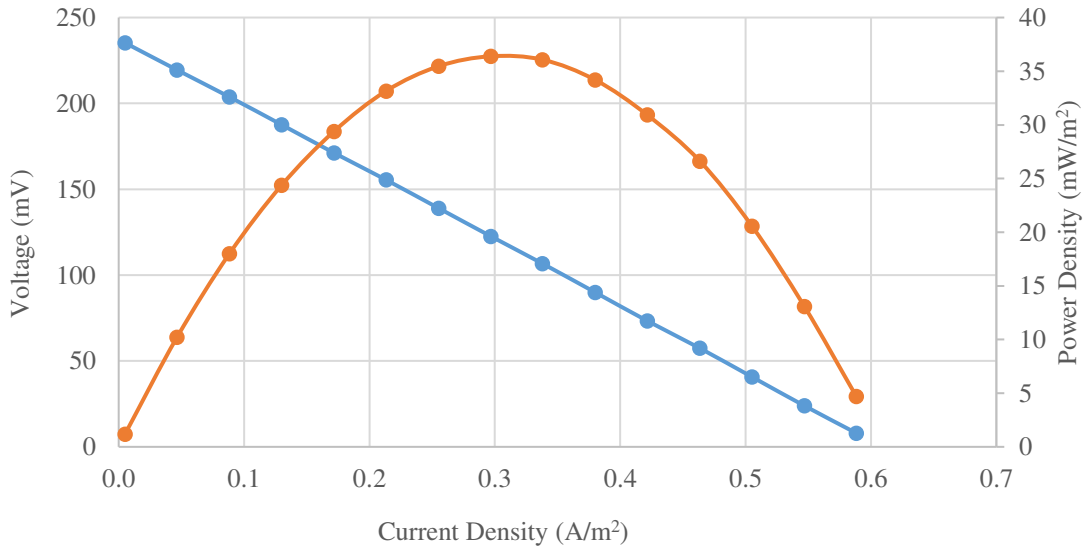

Figure 3: IV curve for microbial fuel cell

Table 1: Comparison of results of the current study with the literature

Substrate	Anode/Cathode	OCV_{max} (V)	COD removal Efficiency (%)	Power Density (mWm^{-2})	Reference
Dairy effluent	Carbon Paste/Carbon Paste	0.396	82	36.39	Present
Soak liquor	Graphite/Graphite	1.069	96	92	(Sathishkumar et al. 2018)
Domestic wastewater	Carbon fiber brush/carbon fiber brush	0.2	78	92	(Logan et al. 2012)
Sewage wastewater	Graphite Rod/Graphite Rod	0.18	82.7	6.73	(Ghangrekar and Shinde 2008)
Distillery wastewater	Graphite Plate/Graphite Rod	0.68	71.8	202	(Samsudeen et al. 2015)
Brewery wastewater	Carbon brush fibers / Activated carbon and PTFE with Pt. catalyst	0.51	20.7	669	(Wen et al. 2010)
Cheese whey	Carbon paper/carbon cloth	N.A	94	46	(Tremouli et al. 2013)

3.3. Electrochemical Impedance Spectroscopy (EIS):

Impedance spectroscopy was performed to study the dynamic response of the electrodes. Figure 4 shows the Nyquist plot of MFC at day 3. The corresponding Bode plot is shown in Figure 5. At least three distinct arcs can be identified from Nyquist and Bode plots; first at higher frequency (between 100 kHz and 500 Hz), second at an intermediate frequency (between 500 Hz and 1 Hz), and third at low frequency (between 1 Hz and 0.04 Hz). The arcs at high and intermediate frequency ranges are expected to originate from the electrode processes and attributed to the anodic and cathodic charge transfer process, respectively. The low-frequency arc proceeds at nearly 45^0 angle in the complex plane that is an indication of the mass transport limitation, therefore, attributed to the diffusional process (Sekar and Ramasamy 2013; Sindhuja et al. 2016).

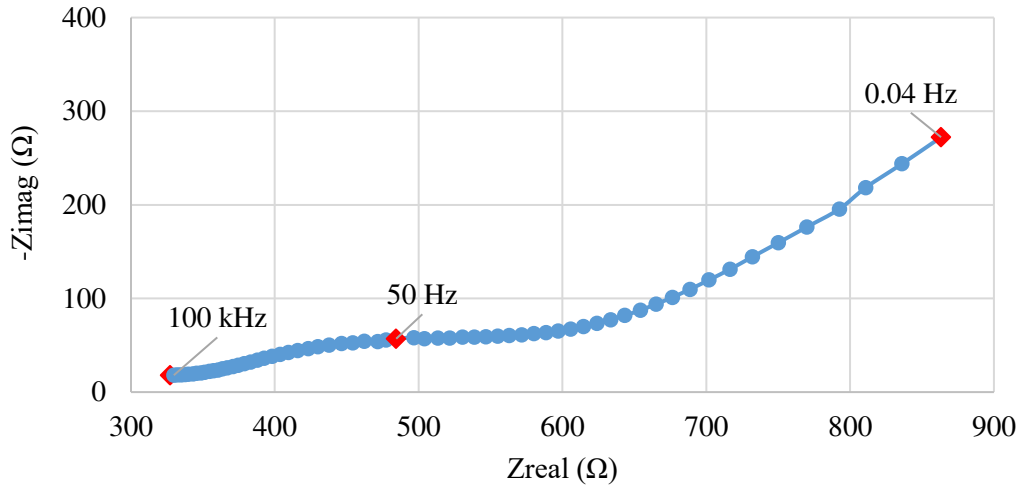

Figure 4: Nyquist plot of MFC at day 3

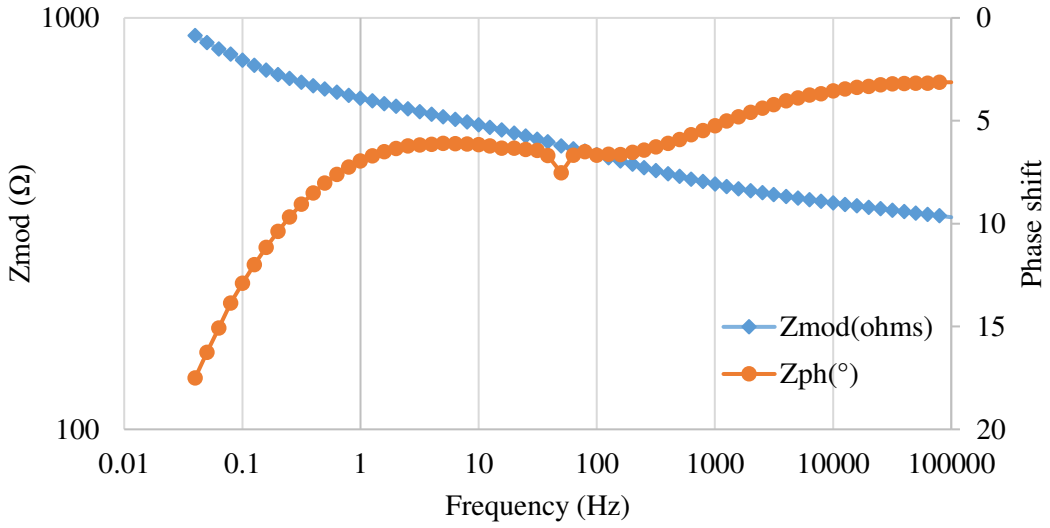

Figure 5: Corresponding Bode plot of MFC at Day 3

Figure 6 compares the impedance response of the cell recorded after day 72 hrs, 168 hrs, 192 hrs, and 240 hrs of the cell manufacturing. To quantify the contribution of each process in the overall resistance, spectra have been fitted to an appropriate equivalent electrical circuit including resistive and capacitive elements. The equivalent circuit model (R_s (R_1CPE_1) (R_2CPE_2W)) used to deconvolute the EIS spectra is shown in Figure 7. In the electrical circuits, R_s corresponds to the internal ohmic resistance arising from the membrane, electrolyte, and metallic connections, R_1 and R_2 correspond to the charge transfer resistances arising from the anode and cathode, respectively. Owing to the distributed capacitive response of the

system, the constant phase elements (CPE_1 and CPE_2) are used here instead of pure capacitors and related to the pseudo-capacitances arising from the corresponding electrochemical interfaces - anode/anolyte and cathode/catholyte, respectively. The mass transport limitation due to ionic diffusion in the solution is given by the infinite Warburg element (W). These key parameters affecting the MFC performance are obtained by fitting the impedance spectra to the circuit model using Echem Analyst software.

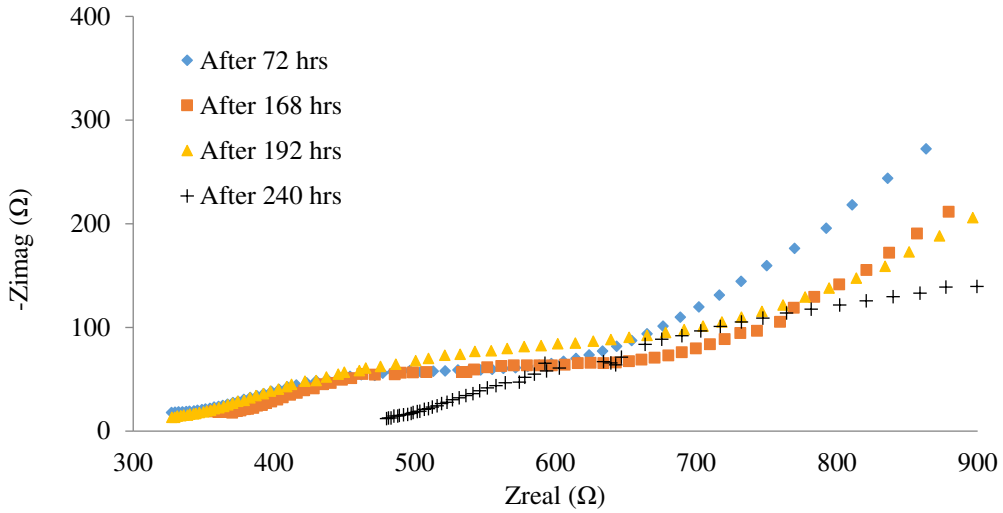

Figure 6: Impedance behavior of the Microbial Fuel Cell during short-term cell operation

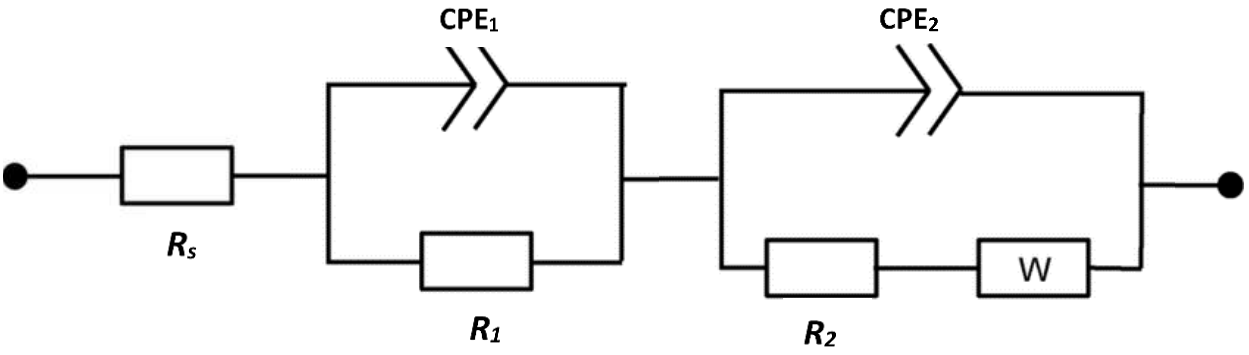

Figure 7: Electrical equivalent circuit for MFC

Table 2 shows the values of equivalent circuit fitting parameters. A consistent order of resistive contribution is found as $R_2 > R_s > R_1$ during 10 days of the cell operation. Clearly, the cathodic polarization resistance contributes maximum to the overall cell resistance followed by ohmic resistance and anodic polarization

resistance. The dominance of the cathodic polarization resistance in such MFC configurations has been observed and reported previously (He et al. 2008; Lepage et al. 2012; Sindhuja et al. 2019). While some studies have also reported the dominance of ohmic resistance (Liang et al. 2007; You et al. 2007; Ramasamy et al. 2008), the same is not reported for anodic polarization resistance in the case of practical dual-chamber MFCs. The value of the ohmic resistance found in this study is comparable to the values reported previously indicating the reasonable conductivity of the electrochemical system.

It is also observed that the anodic polarization resistance (R_1) decreases with time. This drop in the resistance is associated with the microbe film development at the anode surface that has a beneficial effect on the kinetics of the bio-electrochemical reaction. This trend is commonly observed and reported in the MFC literature for at least in the earlier days of the cell operation. For example, Ramasamy et al. (Ramasamy et al. 2008) reported a 40% drop (at 0.27 A/m^2) in the anodic polarization resistance with simultaneous increase of power density by ac. 120% of ferricyanide-cathode MFC during the first five days of the cell operation. Borole et al. (Borole et al. 2010) reported a 75% drop (at 2.63 A/m^2) in the anodic polarization resistance of air-cathode MFC during 70 days of the cell operation. In the present study, ac. A 35% drop in the anodic polarization resistance at the open circuit is observed in merely 10 days. It is worth mentioning that the anolyte pH dropped from 7.62 to 5.8 in 10 days. While it is known that the acidification of the anode biofilm (pH below 7) inhibits the microbial activity and slows down the kinetics of bio-electrochemical reaction (He et al. 2008; Jung et al. 2011), the same is not observed in the present study possibly due to still-developing microbial film. The pseudo-capacitance of the anode is of the orders of μF that rapidly increases with time that also reflects a rapid increase in the charge storage of the anode surface as also reported previously. This can be anticipated while considering the development of biofilm on the anode surface that momentarily holds the charges (electrons) produced during the oxidation process and then delivers to the external circuit. The pseudo-capacitance of the cathode also increases with time possibly due to the accumulation of protons, received from the anode chamber, on the surface of the cathode. The

higher capacitance of the cathode, compared to the anode, also points towards the proton accumulation at the cathode surface attributed to higher resistance of cathode towards oxygen reduction.

The Warburg coefficient (W) that is inversely related to the diffusion coefficients of redox species is also shown in Table 2. As observed, the coefficient value increases with time indicating an increase in the resistance to gas diffusion. The diffusional resistance is typically observed in the aerated cathode MFC designs that are attributed to the oxygen diffusion in the cathodic chamber (Sekar and Ramasamy 2013). Therefore, it is expected that the diffusional resistance observed in this study is also related to the difficulty of oxygen solubilization in the catholyte and subsequent diffusion to the hydrophobic cathode surface.

Table 2: Values of equivalent circuit parameters

Time (hr)	R_s (Ω)	R_1 (Ω)	R_2 (Ω)	CPE (Q_1) x 10^6	CPE(Q_2) x 10^4	W ($S.s^{1/2}$) x 10^3
72	199.2	139.2	281.0	5.14	3.03	5.39
168	216.4	149.7	327.8	6.11	3.53	7.15
192	237.8	106.9	414.5	49.9	5.62	7.77
240	404.2	91.5	784.9	108.1	7.14	10.0

4. Conclusion:

The discharge of untreated dairy effluent containing traces of cow dung pollutes the environment. The present study dealt with the remediation of cow dung and sugar solution and simultaneous power generation. The designed MFC produced a highest of 396 mV of open-circuit voltage and 36.39 mW/m^2 of power density corresponding to 0.30 A/m^2 of current density. Further, 81 % COD removal efficiency and a considerable change in the anolyte PH are observed in 10 days of cell operation. The EIS analysis revealed key information regarding the cell operation. The highest contribution of cathodic polarization resistance to the total internal resistance requires an intelligent selection and design of the cathode in addition to the MEA assembly. Thereby this study demonstrated the dual application i.e. treatment of wastewater and electricity generation.

Ethics approval and consent to participate

Not applicable

Consent for publication

Not applicable

Availability of data and materials

Not applicable

Competing interests

Authors do not have any competing interests.

Funding

This research is supported by the Higher education Commission (HEC) Pakistan through National Research Program for Universities (NRPU # 9594).

Author Contribution:

All authors contributed in this work. **Umair Fazal**: methodology, analysis, and drafting. **Asif N. Tabish**: conceptualization, supervision, editing. **Samina Akbar**: supervision and reviewing. **Iqra Farhat**: Data curation. **Muneeb Irshad**: Validation. **Mohsin Kazmi**: reviewing and editing. **Haider Ali**: reviewing and editing. **Muhammad Irfan**: reviewing and editing

Acknowledgment

Authors are thankful to the Higher education Commission (HEC) Pakistan for funding this work.

References:

Aghababaie M, Farhadian M, Jeihanipour A, Biria D (2015) Effective factors on the performance of microbial fuel cells in wastewater treatment – a review. 2515:. https://doi.org/10.1080/09593330.2015.1077896

Ahn Y, Logan BE (2013) Saline catholytes as alternatives to phosphate buffers in microbial fuel cells. Bioresour Technol 132:436–439. https://doi.org/10.1016/j.biortech.2013.01.113

Bin Z (2009) "Solid oxide fuel cell (SOFC) technical challenges and solutions from nano-aspects." Int J energy Res 31:135–147. https://doi.org/10.1002/er

Borole AP, Aaron D, Hamilton CY, Tsouris C (2010) Understanding long-term changes in microbial fuel cell performance using electrochemical impedance spectroscopy. Environ Sci Technol 44:2740–2745.

https://doi.org/10.1021/es9032937

Call TP, Carey T, Bombelli P, et al (2017) Platinum-free, graphene based anodes and air cathodes for single chamber microbial fuel cells. J Mater Chem A 5:23872–23886. https://doi.org/10.1039/c7ta06895f

Chen Q, Pu W, Hou H, et al (2017) Activated microporous-mesoporous carbon derived from chestnut shell as a sustainable anode material for high performance microbial fuel cells. Elsevier Ltd

Deval A, Dikshit AK (2013) Construction, Working and Standardization of Microbial Fuel Cell. APCBEE Procedia 5:59–63. https://doi.org/10.1016/j.apcbee.2013.05.011

Erable B, Byrne N, Etcheverry L, et al (2017) Single medium microbial fuel cell: Stainless steel and graphite electrode materials select bacterial communities resulting in opposite electrocatalytic activities. Int J Hydrogen Energy 42:26059–26067. https://doi.org/10.1016/j.ijhydene.2017.08.178

Ghangrekar MM, Shinde VB (2008) Simultaneous sewage treatment and electricity generation in membrane-less microbial fuel cell. Water Sci Technol 58:37–43. https://doi.org/10.2166/wst.2008.339

Ghazali NF, Mahmood NABN, Ibrahim KA, et al (2017) Electricity generation from palm oil tree empty fruit bunch (EFB) using dual chamber microbial fuel cell (MFC). IOP Conf Ser Mater Sci Eng 206:. https://doi.org/10.1088/1757-899X/206/1/012025

Gude VG (2016) Wastewater treatment in microbial fuel cells - An overview. J Clean Prod 122:287–307. https://doi.org/10.1016/j.jclepro.2016.02.022

He Z, Huang Y, Manohar AK, Mansfeld F (2008) Bioelectrochemistry Effect of electrolyte pH on the rate of the anodic and cathodic reactions in an air-cathode microbial fuel cell. Bioelectrochemistry 74:78–82. https://doi.org/10.1016/j.bioelechem.2008.07.007

He Z, Mansfeld F (2009) Exploring the use of electrochemical impedance spectroscopy (EIS) in microbial fuel cell studies. Energy Environ Sci 2:215–219. https://doi.org/10.1039/b814914c

Hou B, Hu YY, Sun J, Cao YQ (2010) Effect of anodic biofilm growth on the performance of the microbial fuel cell (MFC). 2010 4th Int Conf Bioinforma Biomed Eng iCBBE 2010 1–4. https://doi.org/10.1109/ICBBE.2010.5514877

Jung S, Mench MM, Regan JM (2011) Impedance characteristics and polarization behavior of a microbial fuel cell in response to short-term changes in medium pH. Environ Sci Technol 45:9069–9074. https://doi.org/10.1021/es201737g

Kim BH, Chang IS, Gadd GM (2007) Challenges in microbial fuel cell development and operation. Appl Microbiol Biotechnol 76:485–494. https://doi.org/10.1007/s00253-007-1027-4

Lepage G, Albernaz FO, Perrier G, Merlin G (2012) Characterization of a microbial fuel cell with reticulated carbon foam electrodes. Bioresour Technol 124:199–207. https://doi.org/10.1016/j.biortech.2012.07.067

Li S, Cheng C, Thomas A (2017) Carbon-Based Microbial-Fuel-Cell Electrodes: From Conductive Supports to Active Catalysts. Adv. Mater. 29

Liang P, Huang X, Fan MZ, et al (2007) Composition and distribution of internal resistance in three types of microbial fuel cells. Appl Microbiol Biotechnol 77:551–558. https://doi.org/10.1007/s00253-007-1193-4

Logan B, Liu H, Oh S-E, Min B (2012) Electricity From Domestic Wastewater Can Be Harvested in Microbial Fuel Cells. Proc Water Environ Fed 2004:581–585.

https://doi.org/10.2175/193864704784147962

Medicado AB (2008) Phosphate Buffered Saline (PBS), pH 7.4 and 7.2 - Product description. 18–19

Moradian JM, Fang Z, Yong Y-C (2021) Recent advances on biomass-fueled microbial fuel cell. Bioresour Bioprocess 8:14. https://doi.org/10.1186/s40643-021-00365-7

Nam JY, Kim HW, Lim KH, et al (2010) Variation of power generation at different buffer types and conductivities in single chamber microbial fuel cells. Biosens Bioelectron 25:1155–1159. https://doi.org/10.1016/j.bios.2009.10.005

Rajasulochana P, Preethy V (2016) Comparison on efficiency of various techniques in treatment of waste and sewage water – A comprehensive review. Resour Technol 2:175–184. https://doi.org/10.1016/j.reffit.2016.09.004

Ramasamy RP, Ren Z, Mench MM, Regan JM (2008) Impact of Initial Biofilm Growth on the Anode Impedance of Microbial Fuel Cells. Biotechnol Bioeng 101:101–108. https://doi.org/10.1002/bit.21878

Ren L, Ahn Y, Logan BE (2014) A two-stage microbial fuel cell and anaerobic fluidized bed membrane bioreactor (MFC-AFMBR) system for effective domestic wastewater treatment. Environ Sci Technol 48:4199–4206. https://doi.org/10.1021/es500737m

Samsudeen N, Radhakrishnan TK, Matheswaran M (2015) Bioelectricity production from microbial fuel cell using mixed bacterial culture isolated from distillery wastewater. Bioresour Technol 195:242–247. https://doi.org/10.1016/j.biortech.2015.07.023

Santoro C, Arbizzani C, Erable B, Ieropoulos I (2017) Microbial fuel cells : From fundamentals to applications . A review. J Power Sources 356:225–244. https://doi.org/10.1016/j.jpowsour.2017.03.109

Sathishkumar K, Narenkumar J, Selvi A, et al (2018) Treatment of soak liquor and bioelectricity generation in dual chamber microbial fuel cell. Environ Sci Pollut Res 25:11424–11430. https://doi.org/10.1007/s11356-018-1371-1

Schröder U (2007) Anodic electron transfer mechanisms in microbial fuel cells and their energy efficiency. Phys Chem Chem Phys 9:2619–2629. https://doi.org/10.1039/b703627m

Sekar N, Ramasamy RP (2013) Electrochemical impedance spectroscopy for microbial fuel cell characterization. J Microb Biochem Technol 5:. https://doi.org/10.4172/1948-5948.s6-004

Sindhuja M, Kumar NS, Sudha V, Harinipriya S (2016) Equivalent circuit modeling of microbial fuel cells using impedance spectroscopy. J Energy Storage 7:136–146. https://doi.org/10.1016/j.est.2016.06.005

Sindhuja M, Sudha V, Harinipriya S (2019) Insights on the resistance, capacitance and bioelectricity generation of microbial fuel cells by electrochemical impedance studies. Int J Hydrogen Energy 44:5428–5436. https://doi.org/10.1016/j.ijhydene.2018.12.075

Slate AJ, Whitehead KA, Brownson DAC, Banks CE (2019) Microbial fuel cells: An overview of current technology. Renew Sustain Energy Rev. https://doi.org/10.1016/j.rser.2018.09.044

Sun J, Li W, Li Y, et al (2013) Redox mediator enhanced simultaneous decolorization of azo dye and bioelectricity generation in air-cathode microbial fuel cell. Bioresour Technol 142:407–414. https://doi.org/10.1016/j.biortech.2013.05.039

Tremouli A, Antonopoulou G, Bebelis S, Lyberatos G (2013) Operation and characterization of a microbial

fuel cell fed with pretreated cheese whey at different organic loads. Bioresour Technol 131:380–389. https://doi.org/10.1016/j.biortech.2012.12.173

Varanasi JL, Veerubhotla R, Das D (2017) Diagnostic tools for the assessment of MFC. Microb Fuel Cell A Bioelectrochemical Syst that Convert Waste to Watts 249–268. https://doi.org/10.1007/978-3-319-66793-5_13

Vu HT, Min B (2019) ScienceDirect Integration of submersible microbial fuel cell in anaerobic digestion for enhanced production of methane and current at varying glucose levels. Int J Hydrogen Energy 1–9. https://doi.org/10.1016/j.ijhydene.2019.01.091

Wang Z, Mei X, Ma J, Wu Z (2012) Recent Advances in Microbial Fuel Cells Integrated with Sludge Treatment. Chem Eng Technol 35:1733–1743. https://doi.org/10.1002/ceat.201200132

Wen Q, Wu Y, Zhao L, Sun Q (2010) Production of electricity from the treatment of continuous brewery wastewater using a microbial fuel cell. Fuel 89:1381–1385. https://doi.org/10.1016/j.fuel.2009.11.004

Yin Y, Huang G, Di M, et al (2017) Increased electroactive species concentration in anodic biofilm of Geobacter-inoculated microbial fuel cells under static magnetic field. Res Chem Intermed 43:873–883. https://doi.org/10.1007/s11164-016-2670-0

You S, Zhao Q, Zhang J, et al (2007) A graphite-granule membrane-less tubular air-cathode microbial fuel cell for power generation under continuously operational conditions. J Power Sources 173:172–177. https://doi.org/10.1016/j.jpowsour.2007.07.063

Zhang Y, Sun J, Hu Y, et al (2012) Bio-cathode materials evaluation in microbial fuel cells : A comparison of graphite felt , carbon paper and stainless steel mesh materials. Int J Hydrogen Energy 37:16935–16942. https://doi.org/10.1016/j.ijhydene.2012.08.064

Figures

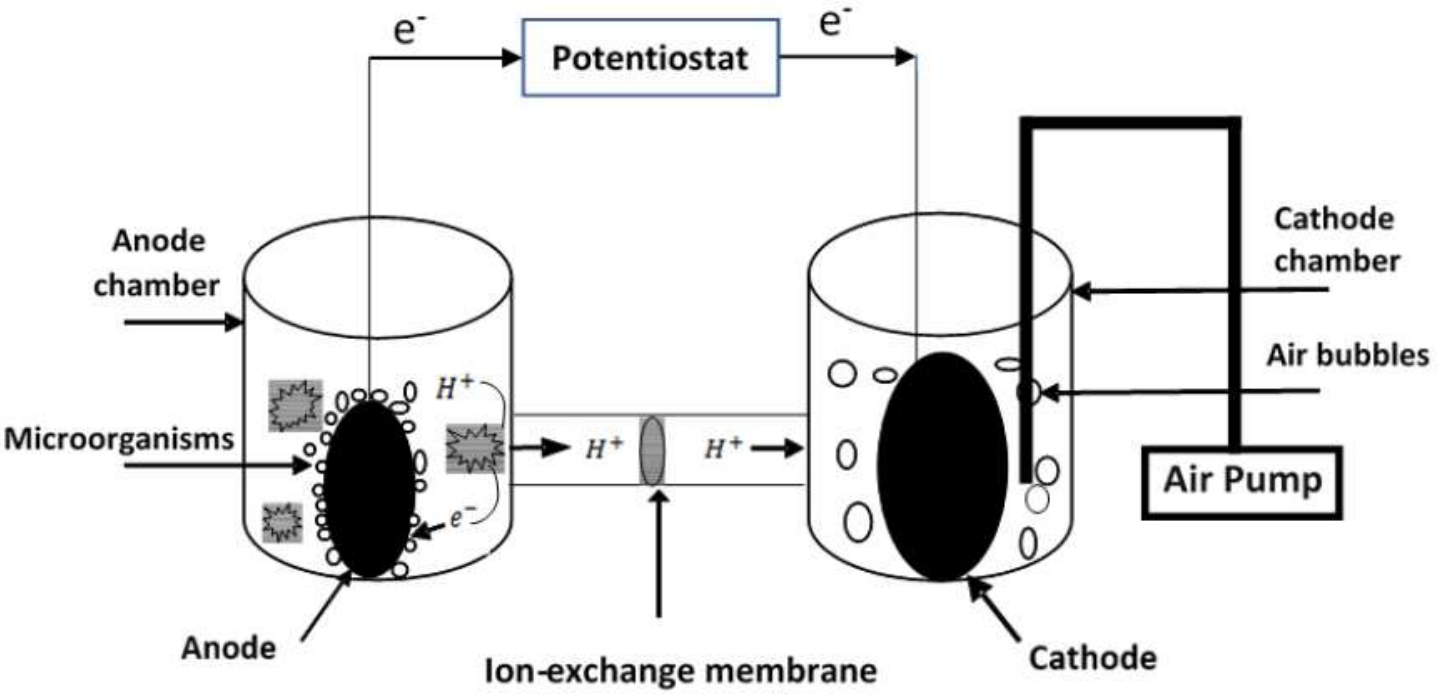

Figure 1

Schematic diagram of Double Chamber Microbial Fuel Cell

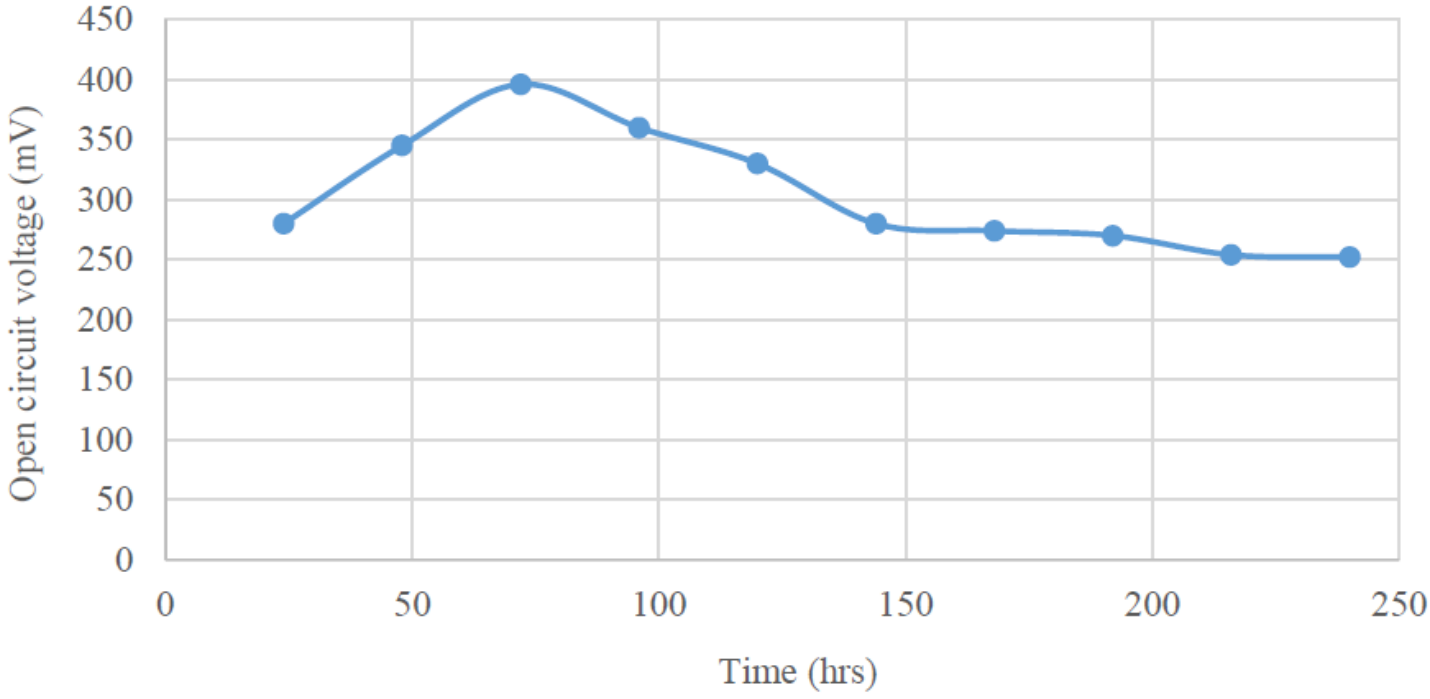

Figure 2

Open circuit voltage

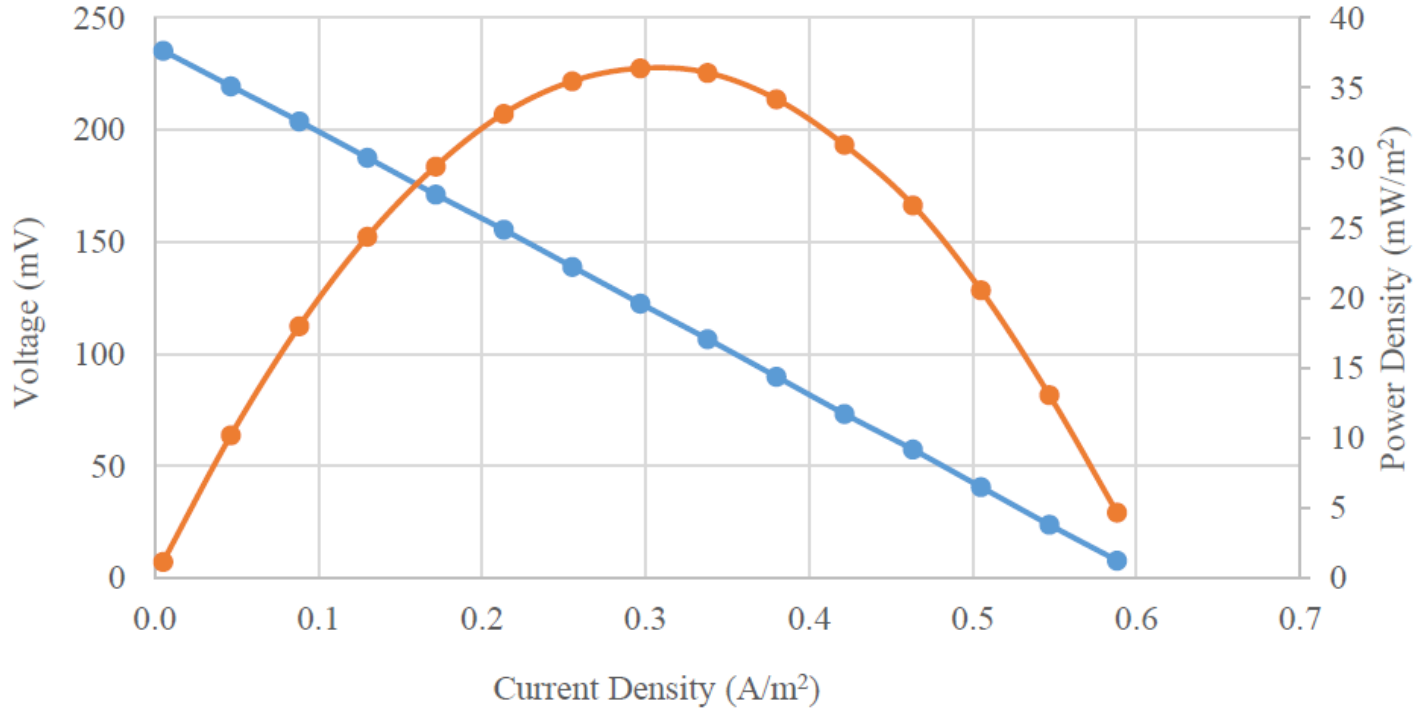

Figure 3

IV curve for microbial fuel cell

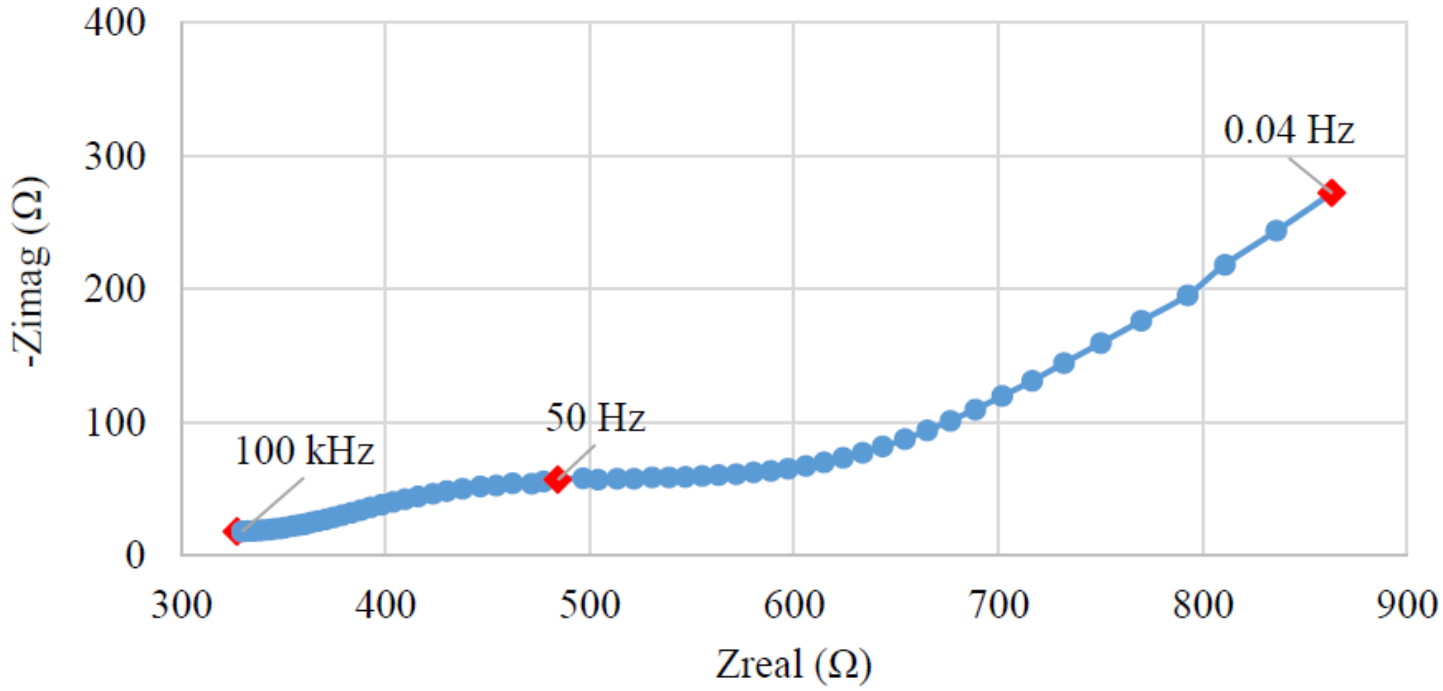

Figure 4

Nyquist plot of MFC at day 3

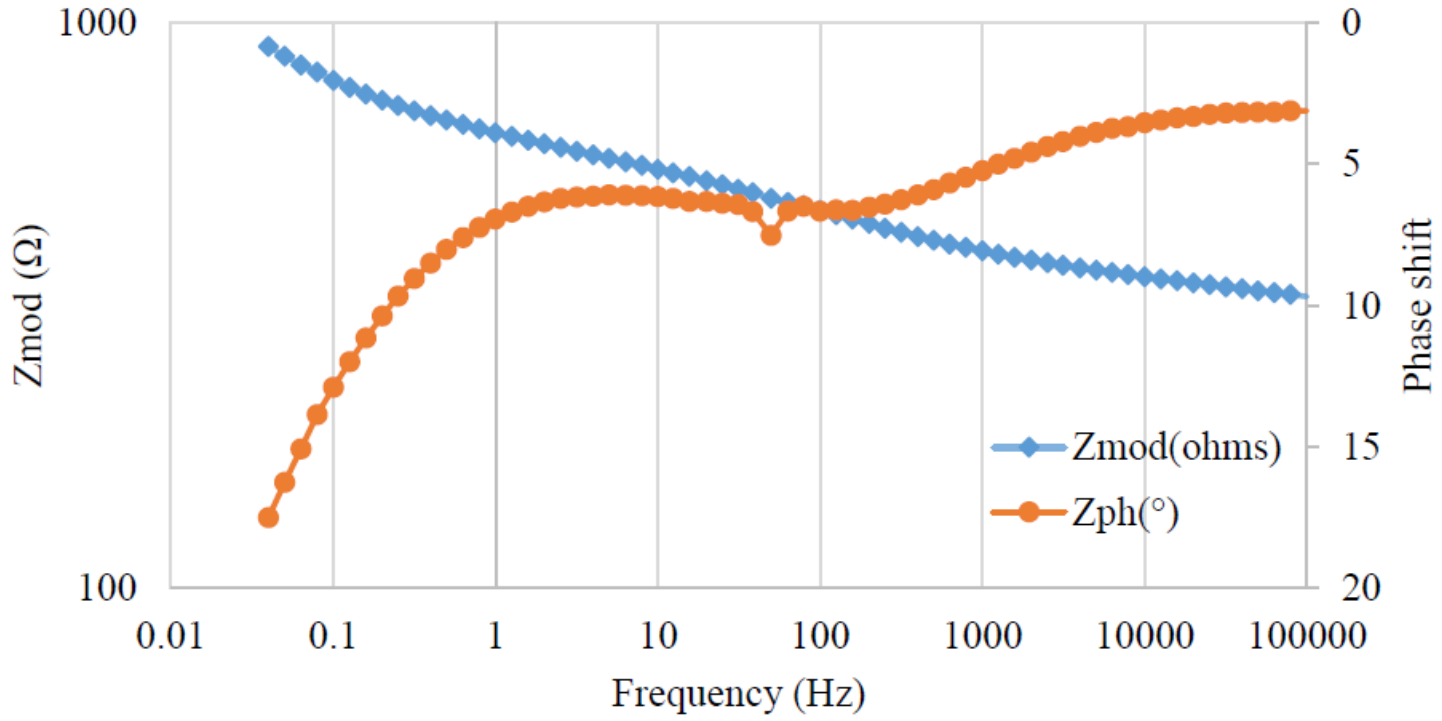

Figure 5

Corresponding Bode plot of MFC at Day 3

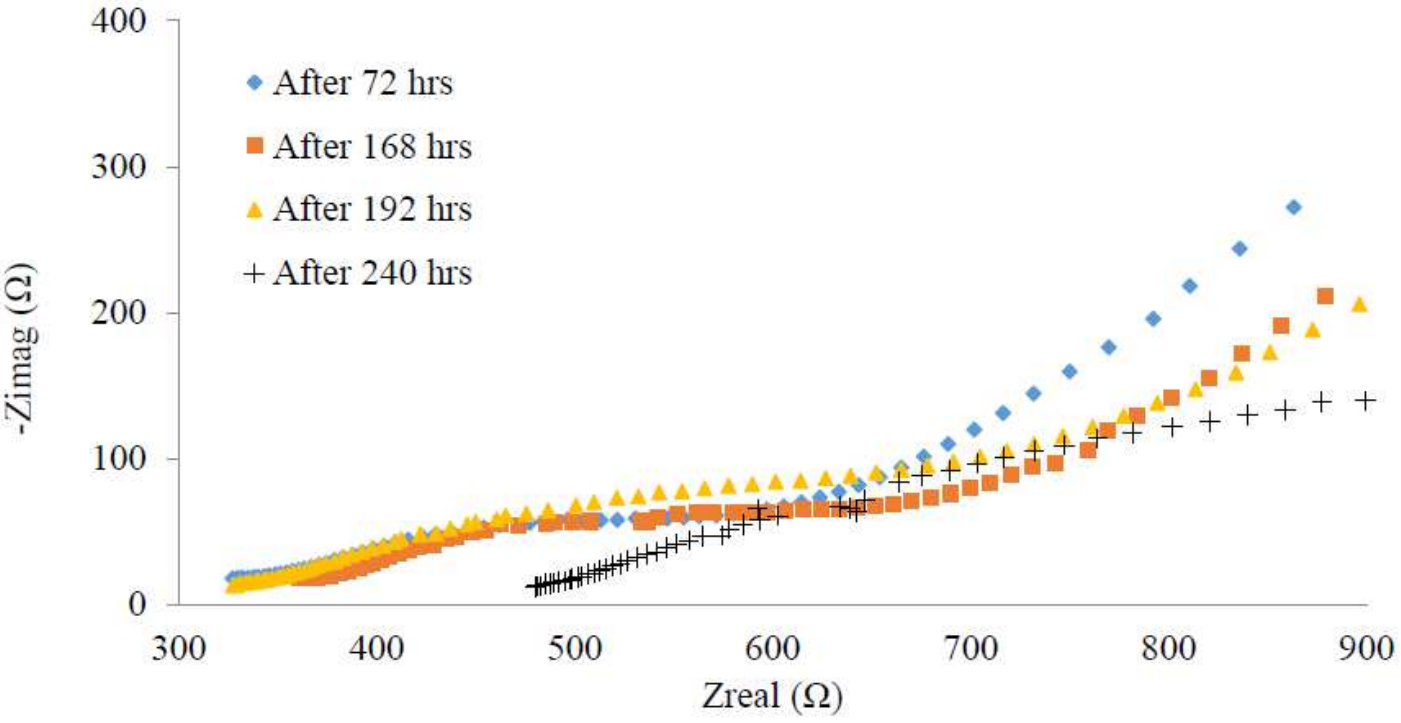

Figure 6

Impedance behavior of the Microbial Fuel Cell during short-term cell operation

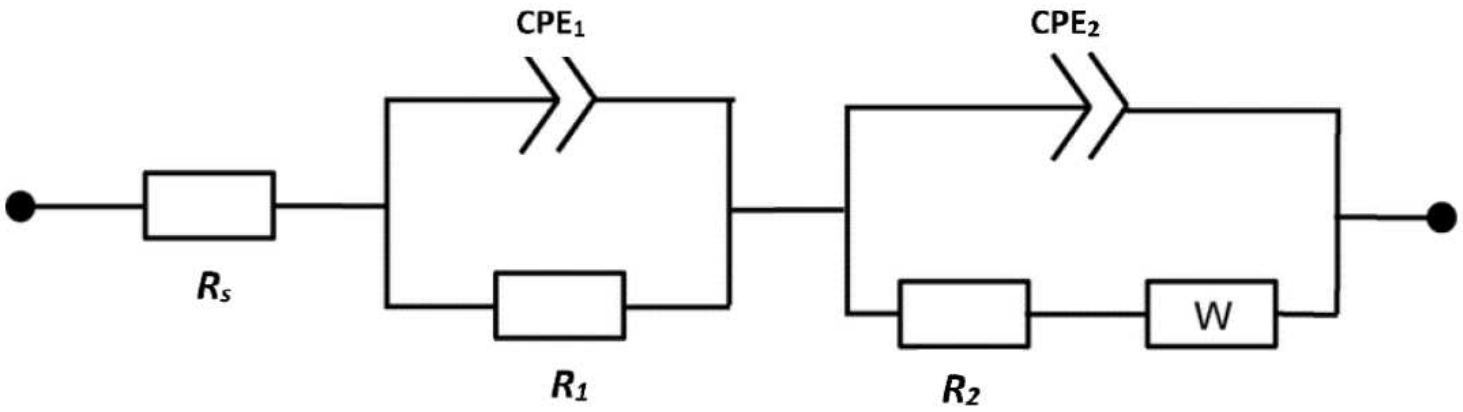

Figure 7

Electrical equivalent circuit for MFC

Supplementary Files

This is a list of supplementary files associated with this preprint. Click to download.

- graphicalabstract.png